UNIVERSIDAD
POLITÉCNICA
DE MADRID

Sensitivity Analysis of Parameter Influence on Thermal Design in UPMSat 3

Study Case 3
MSc in Space Systems

Author: Inés Arauzo Andrés

Tutor: Ignacio Torralbo Gimeno
Javier Piqueras Carreño

Madrid, 9 de marzo de 2024

Contents

List of Figures

List of Tables

Chapter 1

Introduction

In the context of thermal testing, the effectiveness of sensor placement plays an important role in ensuring, not only the accuracy and reliability of test results but also the significance of them. The motivation to improve thermal testing is highlighted by the substantial costs —both in terms of finances and time— associated with thermal testing procedures, which makes even more necessary to get useful results.

Traditional approaches to sensor positioning often fall short in defining thermal experiments due to the complexity of representing the physical processes and properties in a thermal mathematical model. Thus, an adequate parameter selection is key when trying to reduce a thermal mathematical model. This might seem obvious at first sight, but complex thermal mathematical models can have up to thousands of parameters and surpass the million of nodes, so the job of selecting the parameters that capture the physics of the problem for every charge case must not be underestimated.

Throughout this study case we have developed an efficient tool to identify the input parameters that have a significant influence on any of the possible outcomes. This tool has been used on 3 different thermal models in order to get a proper validation:

- A 4 nodes model, which is a simple model where that allows to test the method in a controlled environment.

- A real FPGA model with 8 nodes that is used to test the method in a real, yet simple scenario.

- The UPMSat-3, a real satellite that is currently being developed by the Universidad Politécnica de Madrid. This model is used to test the method in a real scenario.

The results of this work can be applied, in general, to many fields, however the work has been focused on spacecraft and space instruments thermal modeling and testing, in the context of the Space sector. The examples used along the document are centered on space hardware and for that reason, in the next section, the spacecraft thermal control topic is introduced with a brief summary of the particularities of the space environment

1.1 Spacecraft Thermal Control

The thermal design of a spacecraft is primarily influenced by the conditions it encounters during its mission in space. From a thermal perspective, the space environment is characterized by a vacuum, Solar radiation (both direct and reflected by nearby planets, known as albedo), and the infrared emission of celestial bodies.

The main driver of a spacecraft thermal design is the in-flight environment where it needs to operate. From a thermal point of view, the space environment is characterized by the vacuum, the incoming Solar radiation, both direct and reflected by a nearby planet (albedo), and the infrared emission of the planet. Because a spacecraft operates in a vacuum, the only possible thermal interaction between the spacecraft and its environment its through radiation. On an Earth orbit, solar irradiance is the main heat load, with a mean value of 1366 W/m2 and a seasonal variation of $\pm1.7\%$ due to the eccentricity of the orbit of the Earth around the Sun. The solar irradiance value scales with the square of the distance to the Sun, and its spectrum can be modeled, from a thermal point of view, as a black body at some 5762 K, where 99 % of the spectral emissive power of the Sun lies in the range 0.15 to 10 µm wavelength.

1.1.1 Thermal mathematical modelling

When creating a thermal model for an analysis of something space-related, the most common method is the lumped parameters [INSERTAR REFERENCIA], which consist of discretizing the physical system to a finite set of nodes, each of those representing an isotherm tiny volume with some properties associated to itself (with the thermal capacity of the material being among them).

The nodes are interconnected between themselves by the lineal (conductive and convective -if possible-) $G_{L_{ij}}$ and radiative $G_{R_{ij}}$ thermal conductances. The thermal charges are summed up in Q_i (with i being the number of the node); within this term, the solar charge, the planetary albedo, the electrical dissipation of the payloads or the infrared earth emission are

represented among others. Now, using the equation of energy balance,

$$C_i \frac{dT_i}{dt} = Q_i + \sum_{j=1}^{n} G_{Lij} \left(T_j - T_i \right) + \sum_{j=1}^{n} G_{Rij} \sigma \left(T_j^4 - T_i^4 \right) \tag{1.1}$$

we get a system of ordinary differential equations that can be solved through numerical methods.

The values of the thermal conductances and capacitances are not always known, as they are usually a function of physical parameters such as geometry, pressure, torque, or surface finishing. There are several ways of calculating the lineal conductances [REFERENCIA], but when using reduced thermal models (where the geometry has been really simplified) it is usually better to take these G_L as parameters. As for the radiative conductances, G_R, they come from the Geometrical Mathematical Model, the GMM, that is, when defining the geometry of the thermal model, the geometry is also detailed in order to get the external thermal charges and the view factors, which, with the different surface coatings give the corresponding G_R. While the calculation -or at least the estimation- of the G_L can be done analytically and/or experimentally, the G_R are usually obtained numerically through a Monte Carlo analysis [REFERENCIA], as it is quite complex even for relatively simple geometries. Most of the G_L and G_R are calculated through software, however, they usually come from parameters that have been approximated, which is why, in simple models these conductances are often taken as parameters.

1.1.2   Analaysis cases

According to the ECSS, when analyzing the thermal requirements of a space mission, one must evaluate the stationary cold and hot cases first, as they are the most extreme cases, and, if those are properly defined, the temperatures the system might reach will be enveloped by them. This makes the information of these cases really useful.

Furthermore, the fact that these cases are stationary, eliminates the time variance term in Equation 1.1, which means getting the thermal capacitances and its associated uncertainty out of the equation.

This is why this project only focuses on the stationary cases -beginning with the hot and cold charge cases- each defined by a set of boundary conditions BC_K.

Chapter 2

Problem definition

As presented on chapter 1, parameter selection is a key step when creating and/or using models in almost any field, more so, in the space sector where everything has an extra cost associated. However, when talking more specifically about the thermal control for space missions, there are not so many techniques to extract the parameters that define the physics of the problem with most accuracy and observability. This is due to the fact that it has usually been overlooked, never optimizing the amount of information extracted from testing and mission monitoring. Thus, among this chapter the developed method is presented, along with the requirements the system must fulfil in order to use it.

2.1 Algorithm definition

A scheme of the method is developed on Figure 2.1. The method has been implemented on Python [?] using the Pycanha package, a thermal analysis tool developed by Dr.Piqueras that joins a Python front-end with a C+ background in order to get a user-friendly, yet fast thermal solver. All the functions and features created along this project have been implemented as libraries of this package, and can now be obtained open source on GitHub. Apart from pycanha, other commercial libraries such as NumPy [?] and SciPy [?] -For mathematical purposes- and Matplotlib [?] have been used. Throughout the following sections each step of the algorithm is briefly explained.
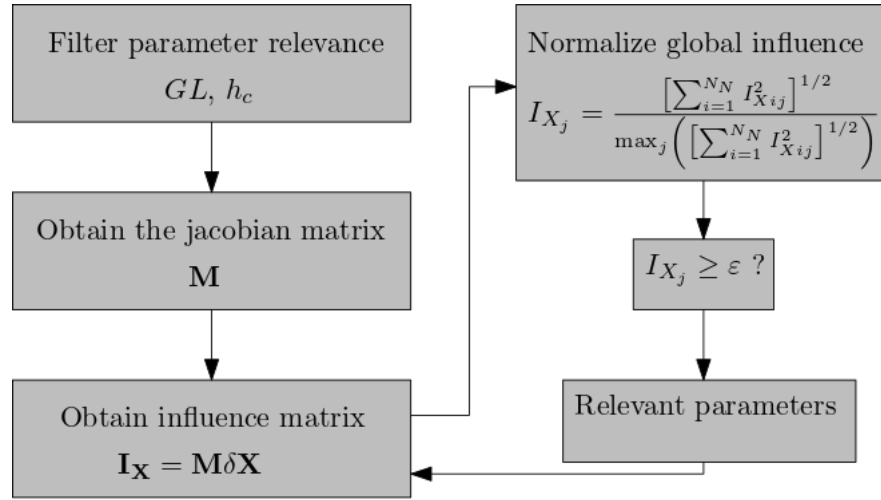
Figure 2.1: Flow diagram of the method algorithm

2.2 Data Read

The first step of the method consist of the acquisition of data, whether it comes from an external model or if it has been developed directly with Pycanha. This second option is way easier, as the data read would be as easy as reading the TMM object, and all the parameters, associated formulas, geometrical definition etc. would be known. However, as pycanha is still on development it is quite difficult to create any kind of complex system, due to the lack of a graphic interface to create the geometry.

In order to make the package more usable with regard to bigger projects, the compatibility with the most extended spacecraft thermal analysis tool, ESATAN-TMS [?], is provided within the package. The files that pycanha uses to replicate the model created in esatan are the .TMD and some of the .data files, which must be exported separately.

The .TMD files are binary coded files that result from each charge case, and they contain all the necessary information to run a TMM. These files give directly the lineal and radiative coupling matrices K and R, the thermal capacities C and the boundary conditions Q, and with that the system of equations presented on Equation 1.1, can be solved.

However, this just gives the numerical result, eliminating all the parameters and formulas that are associated to the calculations of these matrices, which would not be useful to make any kind of analysis, so they have to be overwritten. Thus, after reading the .TMD, the .CONSTANTS.data and .LOCALS.data are read first and then, once the TMM has the parameters, the formulas are read in .COUPLINGS.data.

To summarize:

- Create an empty TMM object.

- Read the .TMD file with all the numerical data.

- Read the parameters files.

- Overwrite de conductances gotten from the .TMD with the formulas associated to the arameters.

2.3   Manual filter

Once all the data has been read, the engineer has to choose an initial set of parameters to begin the analysis with. This task must be done manually as it is not a matter of influence or sensitivity but the kind of parameters one wants to study. It takes not only an important engineering knowledge but also a great understanding of the model itself to be able to select an optimum set of parameters.

It will be further explained on latter chapters, but these choices are way easier to make if the model is developed by the same person who makes the analysis, as the parametrization will be purposefully done in a way that simplifies this task; this is the case for the 2 first cases that are analyzed, where due to this (and to the simpliccity of the models), this step can be skipped. However, in the third case, the UPMSat3 model is way more complex than the other two example cases and furthermore, it has been developed by a different person who had no idea of the purpose of this parametrization, which highlights the importance of this step.

However, for the proposed analysis, the materials and coatings do not change, and thus, neither does the thermo-optical properties, the densities or the conductivities associated to them. The radiative conductances were not even parametrized in first place, but as the thermo-optical properties do not change and neither does the geometry, they will not be part of this initial set. Other parameters such as TIME or PERIOD do not variate either so can also be excluded. Furthermore, as previously mentioned, the study does not take into account the time variation, it is stationary, and thus the thermal capacities, have been also excluded.

Taking this filter into account, the final list must mainly comprehend lineal conductances G_L, or alternatively the h_c.

2.4 Jacobian matrix calculation

The algorithm uses the influence matrix to find which parameters have most influence on which nodes. In order to do that, it is necessary to calculate the Jacobian or Sensitivity matrix $\boldsymbol{M_t}$, defined by the derivatives of the temperature T_i at each node with respect to each parameter p_j,

$$\boldsymbol{M_t} = \frac{\partial T_i}{\partial p_j} = \begin{bmatrix} \frac{\partial T_1}{\partial p_1} & \frac{\partial T_1}{\partial p_2} & \cdots & \frac{\partial T_1}{\partial p_{N_P}} \\ \cdots & \cdots & & \cdots \\ \frac{\partial T_{N_N}}{\partial p_1} & \frac{\partial T_{N_N}}{\partial p_2} & \cdots & \frac{\partial T_{N_N}}{\partial p_{N_P}} \end{bmatrix}. \tag{2.1}$$

For simpler models, such as the 4 nodes one, the Jacobian can be obtained analytically, but in general there is no analytical solution, and it must be computed numerically. Thus, the approach has been to approximate these derivatives by central finite differences[1].The central difference approximation for the partial derivative $\frac{\partial T_i}{\partial p_j}$ is given by:

$$\frac{\partial T_i}{\partial p_j} \approx \frac{T_i(p_j + \Delta p_j) - T_i(p_j - \Delta p_j)}{2\Delta p_j} \tag{2.2}$$

Here, Δp_j is a small perturbation applied to the parameter p_j. The central difference method is chosen because it provides a more accurate approximation of the derivative compared to forward or backward differences, especially when dealing with numerical computations.

To determine the appropriate perturbation Δp_j for each parameter p_j,the following expression is used:

$$\Delta p_j = p_j \cdot \sqrt{\varepsilon} \tag{2.3}$$

where ε is the machine epsilon for floating-point arithmetic, meaning the upper bound on the relative error due to rounding in floating-point calculations. In Python, this can be obtained using `epsilon = np.finfo(float).eps`

The perturbation Δp_j is chosen as a small fraction of the parameter p_j itself, scaled by the square root of the machine epsilon. This ensures that the perturbation is neither too large (which could lead to inaccurate approximations due to nonlinear effects) nor too small (which could result in numerical inaccuracies due to round-off errors).

To summarize, the computation of the Jacobian matrix $\boldsymbol{M_t}$ using central differences can be written as:

---

[1]The options of forward and backward differences have also been implemented

$$(\boldsymbol{M_t})_{ij} = \frac{T_i(p_j + \Delta p_j) - T_i(p_j - \Delta p_j)}{2\Delta p_j}, \tag{2.4}$$

with

$$\Delta p_j = p_j \cdot \sqrt{\varepsilon}, \tag{2.5}$$

ensuring a balanced trade-off between accuracy and numerical stability in the computation of the derivatives.

2.5 Linear dependence filter

With the Jacobian matrix properly calculated, a second filter is applied. Within this step, the intention is to eliminate the parameters that are linearly dependent among themselves. In order to see this dependence, the Pearson correlation coefficient matrix is used. These coefficients measure the linear correlation between two variables, returning a value between -1 and +1. The closest the value of the coefficient is to +1 or -1, the more linearly dependent those values are, either directly (+1) or inversely (-1).

For a dataset with p variables (in this case the parameters, disposed as columns of the Jacobian matrix), the Pearson correlation coefficient matrix $\mathbf{R}$ is a $p \times p$ matrix where each element r_{ij} is the Pearson correlation coefficient between the i-th and j-th variables.

Given a data matrix $\mathbf{M}$ of size $n \times p$, where n is the number of observations (in this case nodes), the Pearson correlation coefficient matrix can be computed as follows:

First, the data matrix $\mathbf{M}$ is standardized to have zero mean and unit variance:

$$\mathbf{Z} = \frac{\mathbf{M} - \mu}{\sigma},$$

where μ is a vector of means and σ is a vector of standard deviations for each parameter.

Then, the Pearson correlation coefficient matrix $\mathbf{R}$ is calculated as:

$$\mathbf{R} = \frac{1}{n-1}\mathbf{Z}^\top \mathbf{Z},$$

which, in matrix notation, can be written as:

$$\mathbf{R} = \begin{bmatrix} 1 & r_{12} & \cdots & r_{1p} \\ r_{21} & 1 & \cdots & r_{2p} \\ \vdots & \vdots & \ddots & \vdots \\ r_{p1} & r_{p2} & \cdots & 1 \end{bmatrix},$$

where each r_{ij} is computed using the standardized data matrix $\mathbf{Z}$.

The Pearson correlation coefficient r_{ij} between the i-th and j-th variables can also be expressed in terms of the dot product of their standardized values:

$$r_{ij} = \frac{\sum_{k=1}^{n}(z_{ik}z_{jk})}{n-1},$$

where z_{ik} and z_{jk} are the k-th observations of the i-th and j-th standardized variables, respectively.

Taking the absolute value of this matrix $|\,\mathbf{R}\,|$, we have a diagonal and symmetrical matrix with values going from 0 to $+1$, (with the main diagonal filled with ones) where the closest a value is to 1, the more linearly related are the corresponding parameters. Thus, a correlation threshold ε_{LD} is set around 0.997, and whenever any pair of parameters is higher than the threshold, one parameter of the pair is eliminated.

After that, the columns corresponding to those parameters p_{LD} are eliminated from the Jacobian matrix, resulting in a reduced matrix M_{LI}, standing for linearly independent.

2.6   Influence matrix and normalization

In order to choose the most adequate parameters to determine the reduced model, the matrix of influence $\mathbf{I_X}$ is defined below:

$$\mathbf{I_X} = \begin{bmatrix} \frac{\partial T_1}{\partial p_1}\delta p_1 & \frac{\partial T_1}{\partial p_2}\delta p_2 & \cdots & \frac{\partial T_1}{\partial p_{N_P}}\delta p_{N_P} \\ \ldots & \ldots & & \ldots \\ \frac{\partial T_{N_N}}{\partial p_1}\delta p_1 & \frac{\partial T_{N_N}}{\partial p_2}\delta p_2 & \cdots & \frac{\partial T_{N_N}}{\partial p_{N_P}}\delta p_{N_P} \end{bmatrix} = \mathbf{M}\delta\boldsymbol{P} \qquad (2.6)$$

where $\mathbf{M_t}$ is the jacobian or sensibility matrix defined in the previous section, and $\delta\boldsymbol{P}$ is a vector containing the allowable variation of each parameter within the design. In the influence matrix $\mathbf{I_X}$ each column represents the temperature variation of the nodes that would be generated by a deviation on the parameter δp_i. Therefore, the elements of this matrix have dimensions of temperature, showing the effect of every parameter in the model,

which would not be possible using the jacobian matrix directly.

Preliminarly, the parameter deviation $\delta \boldsymbol{P}$ was taken as a 10% deviation of the parameters, as at first the real allowable deviation was not available. It is interesting to see the change in the results between both of these deviations (see Chapter 5) as it shows the importance of using the influence matrix instead of just the jacobian. Representations of influence matrices will be seen and analyzed in latter chapters, for example in METER REFERENCIA.

Each influence matrix show the effect of varying each one of the parameters has on the structure in terms of temperature, giving an easy visible relation of the importance of each parameter and where it can be measured. However, in order to choose which parameters to continue with, the influence is normalized as follows:

$$I_{X_j} = \frac{\left[\sum_{i=1}^{N_N} I_{Xij}^2 \right]^{1/2}}{max_j \left(\left[\sum_{i=1}^{N_N} I_{Xij}^2 \right]^{1/2} \right)}, \tag{2.7}$$

where I_{Xij} are the values of the influence matrix $\boldsymbol{I_X}$. This way it is easier to see the impact each parameter has on the model, and then choose the most optimal ones to run the tests.

2.7 FPGA model

An FPGA, or Field-Programmable Gate Array, is a type of electronic device that can be programmed by the user after it has been manufactured. This means that an FPGA can be configured to perform a wide variety of tasks, making it very versatile and very useful for space missions. However, they usually have a simple and very similar disposition of components, which makes them easy to thermally model.

In this case, the thermal model disposition is based on the one in REFERENCIA FPGA, and it has been represented on REFERENCIA IMAGEN FPGA.
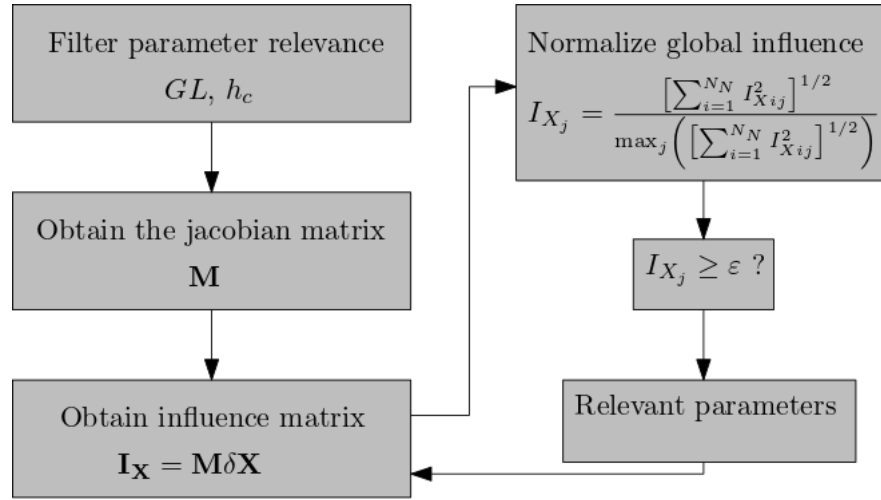
Figure 2.2

Here, in the following table, the nodes are named in order to explain and clarify the model and the dissipation of each of them is also defined,

Table 2.1

Node Number	Structure Part	Q_I [W]
1	Board	3
2	Junction	0
3	Case	0
4	Heat sink	0
5	Strap joint	0
6	Structure A	0
7	PCB frame	0
9	Environment	0

As can be seen in **??**, the radiation is considered at two nodes only; in the Board one, since the temperature difference with the environment reaches its peak here, and in node 4, as the main purpose of the heat sink is to radiate heat to the environment. The rest of the structure is radiatively ignored due to the small size of the visible areas and the simplicity of the model. Apart from this, the environment temperature was set to 293.15 K.

Having been above-mentioned, this model was directly developed with the pycanha package, with the main purpose of using this method, which is why the parameters that define the model are all G_Ls. Thus, the first step of manually selecting these conductances can be

skipped. The parameters are presented in Table 2.2 below:

Table 2.2

Parameter	Description	Value[W]
GL_{12}	Conductance between the board and the junction	0.5
GL_{23}	Conductance between the junction and the case	2
GL_{34}	Conductance between the case and the Heat sink	0.2
GL_{45}	Conductance between the Heat sink and the thermal strap joint	0.15
GL_{56}	Conductance between the thermal strap joint and the structure	0.15
GL_{17}	Conductance between the Board and the Board frame	0.4
GL_{76}	Conductance between the Board frame and the Structure	0.4

Again, as the initial list does not compel any extra parameter (optical properties, conductivities, thermal capacities etc.) the initial list of parameters is the one in Table 2.2. Thus, we can proceed to calculate the jacobian matrix.

The Jacobian matrix result is presented in

$$
\boldsymbol{J} = \left[\begin{pmatrix}
7.63 \cdot 10^{-6} & -2.37 \cdot 10^{0} & -1.36 \cdot 10^{0} & -1.18 \cdot 10^{0} & -1.58 \cdot 10^{1} & -8.39 \cdot 10^{-4} & -3.24 \cdot 10^{-4} \\
0.00 \cdot 10^{0} & 2.64 \cdot 10^{0} & -1.00 \cdot 10^{0} & -1.66 \cdot 10^{0} & -2.21 \cdot 10^{1} & -1.22 \cdot 10^{-3} & -4.67 \cdot 10^{-4} \\
0.00 \cdot 10^{0} & 2.41 \cdot 10^{0} & -9.13 \cdot 10^{-1} & 1.20 \cdot 10^{0} & -2.37 \cdot 10^{1} & -1.30 \cdot 10^{-3} & -4.96 \cdot 10^{-4} \\
0.00 \cdot 10^{0} & 4.11 \cdot 10^{-2} & -1.56 \cdot 10^{-2} & 2.06 \cdot 10^{-2} & 2.74 \cdot 10^{-1} & -2.16 \cdot 10^{-3} & -8.30 \cdot 10^{-4} \\
7.63 \cdot 10^{-6} & 2.05 \cdot 10^{-2} & -7.79 \cdot 10^{-3} & 1.03 \cdot 10^{-2} & 1.37 \cdot 10^{-1} & 1.71 \cdot 10^{-1} & -6.51 \cdot 10^{-2} \\
7.63 \cdot 10^{-6} & 9.54 \cdot 10^{-6} & 3.81 \cdot 10^{-6} & 5.72 \cdot 10^{-5} & 5.09 \cdot 10^{-5} & 2.54 \cdot 10^{-5} & 0.00 \cdot 10^{0} \\
7.63 \cdot 10^{-6} & -1.18 \cdot 10^{0} & 4.49 \cdot 10^{-1} & -5.92 \cdot 10^{-1} & -7.89 \cdot 10^{0} & -4.07 \cdot 10^{-4} & -1.62 \cdot 10^{-4}
\end{pmatrix} \right],
$$

$$(2.8)$$

this matrix does not really throw us much information, but following the procedure from section 2.5, one can calculate the Pearson Correlation Coefficients Matrix, getting the following matrix:

$$
\boldsymbol{R} = \left[\begin{pmatrix}
1.0 & -6.9058 \cdot 10^{-1} & 2.1059 \cdot 10^{-1} & -2.0384 \cdot 10^{-1} & 2.8079 \cdot 10^{-1} & 3.8368 \cdot 10^{-1} & -3.7221 \cdot 10^{-1} \\
-6.9058 \cdot 10^{-1} & 1.0 & -2.1383 \cdot 10^{-1} & 2.4005 \cdot 10^{-1} & -4.5252 \cdot 10^{-1} & -4.6117 \cdot 10^{-2} & 3.8611 \cdot 10^{-2} \\
2.1059 \cdot 10^{-1} & -2.1383 \cdot 10^{-1} & 1.0 & 2.8671 \cdot 10^{-1} & 7.9104 \cdot 10^{-1} & 2.2341 \cdot 10^{-1} & -2.1606 \cdot 10^{-1} \\
-2.0384 \cdot 10^{-1} & 2.4005 \cdot 10^{-1} & 2.8671 \cdot 10^{-1} & 1.0 & 1.9556 \cdot 10^{-1} & 1.3120 \cdot 10^{-1} & -1.3233 \cdot 10^{-1} \\
2.8079 \cdot 10^{-1} & -4.5252 \cdot 10^{-1} & 7.9104 \cdot 10^{-1} & 1.9556 \cdot 10^{-1} & 1.0 & 3.4234 \cdot 10^{-1} & -3.3551 \cdot 10^{-1} \\
3.8368 \cdot 10^{-1} & -4.6117 \cdot 10^{-2} & 2.2341 \cdot 10^{-1} & 1.3120 \cdot 10^{-1} & 3.4234 \cdot 10^{-1} & 1.0 & -9.9971 \cdot 10^{-1} \\
-3.7221 \cdot 10^{-1} & 3.8611 \cdot 10^{-2} & -2.1606 \cdot 10^{-1} & -1.3233 \cdot 10^{-1} & -3.3551 \cdot 10^{-1} & -9.9971 \cdot 10^{-1} & 1.0
\end{pmatrix}\right], \tag{2.9}
$$

where the values of r_{57}, r_{12} and r_{75} are above the ε_{LD}, thus making these parameters linearly dependent. We have chosen to retain only GL_{12}, due to the importance of that parameter.

With the lineally dependent parameters chosen, the new reduced Jacobian is expressed as,

$$
\boldsymbol{J_{LI}} = \left[\begin{pmatrix}
7.63 \cdot 10^{-6} & -2.37 \cdot 10^{0} & -1.36 \cdot 10^{0} & -1.18 \cdot 10^{0} & -8.39 \cdot 10^{-4} & -3.24 \cdot 10^{-4} \\
0.00 \cdot 10^{0} & 2.64 \cdot 10^{0} & -1.00 \cdot 10^{0} & -1.66 \cdot 10^{0} & -1.22 \cdot 10^{-3} & -4.67 \cdot 10^{-4} \\
0.00 \cdot 10^{0} & 2.41 \cdot 10^{0} & -9.13 \cdot 10^{-1} & 1.20 \cdot 10^{0} & -1.30 \cdot 10^{-3} & -4.96 \cdot 10^{-4} \\
0.00 \cdot 10^{0} & 4.11 \cdot 10^{-2} & -1.56 \cdot 10^{-2} & 2.06 \cdot 10^{-2} & -2.16 \cdot 10^{-3} & -8.30 \cdot 10^{-4} \\
7.63 \cdot 10^{-6} & 2.05 \cdot 10^{-2} & -7.79 \cdot 10^{-3} & 1.03 \cdot 10^{-2} & 1.71 \cdot 10^{-1} & -6.51 \cdot 10^{-2} \\
7.63 \cdot 10^{-6} & 9.54 \cdot 10^{-6} & 3.81 \cdot 10^{-6} & 5.72 \cdot 10^{-5} & 2.54 \cdot 10^{-5} & 0.00 \cdot 10^{0}
\end{pmatrix}\right], \tag{2.10}
$$

Following the algorithm, the reduced Jacobian matrix is used to obtain the influence matrix. In this case, the deviation used to compute this matrix was taken from REFERENCIA, and it can be seen on Table 2.3

Table 2.3

Parameter number	Name	Deviation
1	GL_{12}	0.05
2	GL_{23}	0.04
3	GL_{34}	0.20
4	GL_{45}	0.02
5	GL_{56}	0.01
6	GL_{17}	0.01
7	GL_{76}	0.04

The resulting influence matrix is:

$$
\boldsymbol{I_{red}} =
\begin{pmatrix}
2.7249 \cdot 10^{-1} & 1.7781 \cdot 10^{-1} & 3.8147 \cdot 10^{-7} & 2.4882 \cdot 10^{-1} & 2.7247 \cdot 10^{-1} \\
2.0065 \cdot 10^{-1} & 3.0645 \cdot 10^{-1} & 7.6294 \cdot 10^{-7} & 1.6752 \cdot 10^{-1} & 2.0064 \cdot 10^{-1} \\
1.8269 \cdot 10^{-1} & 2.7902 \cdot 10^{-1} & 7.6294 \cdot 10^{-7} & 2.0678 \cdot 10^{-1} & 1.8268 \cdot 10^{-1} \\
3.1155 \cdot 10^{-3} & 4.7585 \cdot 10^{-3} & 7.6294 \cdot 10^{-7} & 3.5278 \cdot 10^{-3} & 3.0830 \cdot 10^{-3} \\
1.5579 \cdot 10^{-3} & 2.3796 \cdot 10^{-3} & 7.6294 \cdot 10^{-7} & 1.7647 \cdot 10^{-3} & 4.1271 \cdot 10^{-3} \\
3.8147 \cdot 10^{-7} & 0.0000 \cdot 10^{0} & 3.8147 \cdot 10^{-7} & 3.8147 \cdot 10^{-7} & 0.0000 \cdot 10^{0} \\
3.6228 \cdot 10^{-1} & 3.1494 \cdot 10^{-1} & 4.5207 \cdot 10^{-1} & 3.5044 \cdot 10^{-1} & 3.6227 \cdot 10^{-1}
\end{pmatrix} .,
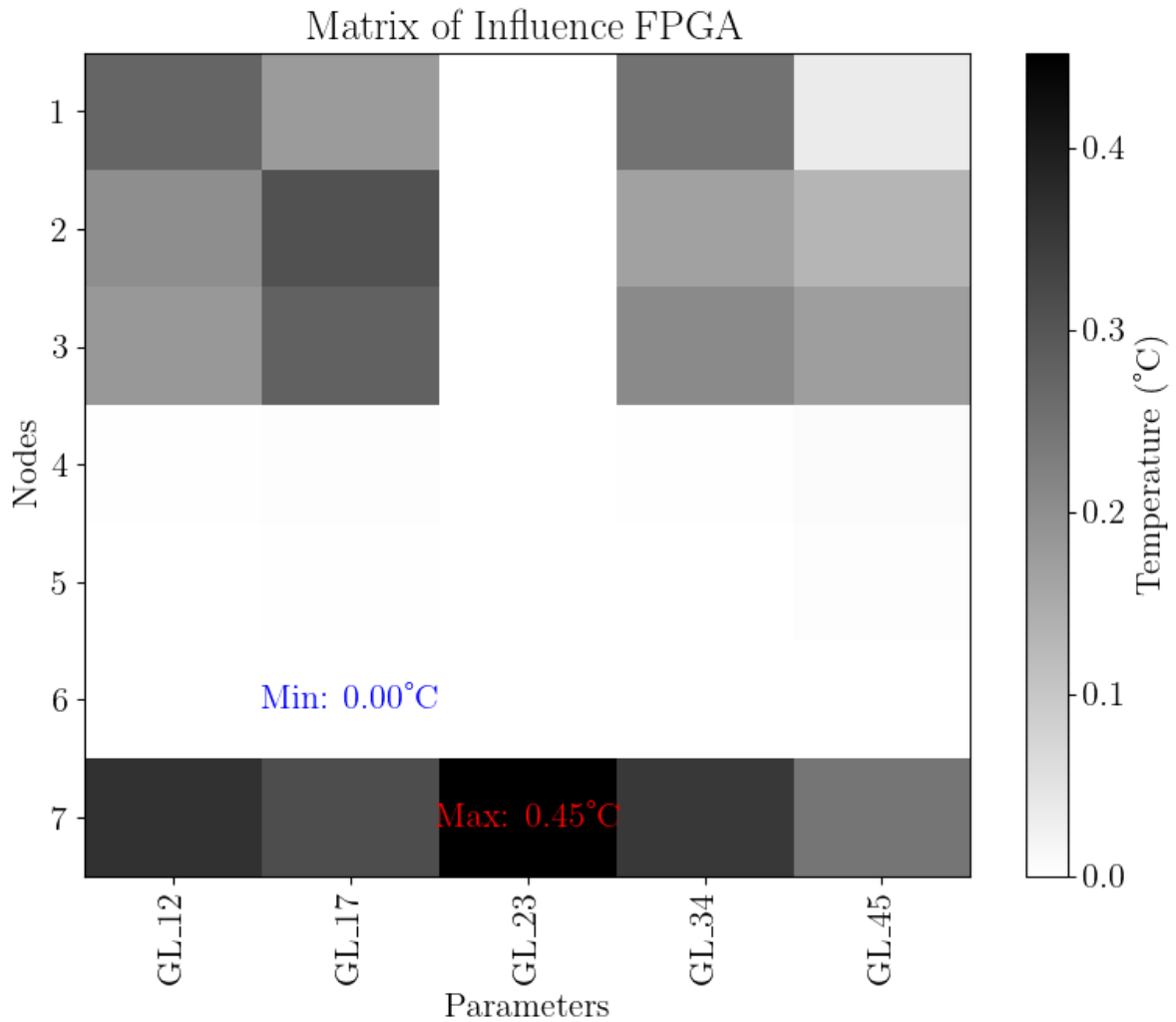\tag{2.11}
$$

which is graphically presented in Figure 2.3

Figure 2.3: Influence matrix of the FPGA

In Figure 2.3 it can be seen that the most important parameters are GL_ and GL_, and the points where they reach its maximum are nodes PATATIN and PATATON. However, in order to consider the influence of the parameters among all the nodes of the model, they are normalized. The result of this normalization can be seen in Figure 2.4
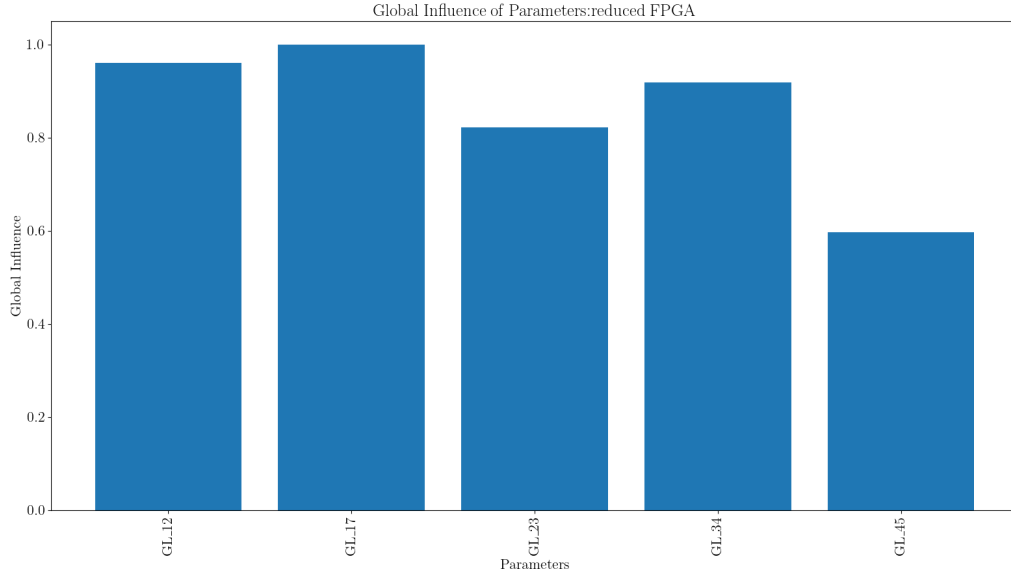

Figure 2.4: Normalized global influence of the parameters of the FPGA

Setting the influence threshold on $\varepsilon_I = 0.1$, no parameter can be eliminated.

Finally, the parameters that are chosen to study the FPGA model are:

Table 2.4: Final Parameters chosen for the FPGA model

Parameter number	Name	Value
1	GL_{12}	0.5
2	GL_{23}	0.4
3	GL_{34}	2.0
4	GL_{45}	0.2
6	GL_{17}	0.1

Take into account that even though this is a really simple model and this process here looks unnecessary, as there are just 9 initial parameters, this is just an explanation; in the next chapter we will be analyzing a real complex model and the importance of following a standard procedure will come clear.

Chapter 3

Application to the UPMSat3

3.1   Introduction

The UPMSat-3 is a university satellite project led by the "Instituto Universitario de Microgravedad Ignacio Da Riva" (IDR/UPM), a research institute from the Universidad Politécnica de Madrid (UPM). It is being developed in collaboration with the Real-Time Systems research group from UPM (STRAST, Sistemas de Tiempo Real y Arquitectura de Servicios Telemáticos). The UPMSat-3 is characterized as a 12U CubeSat with $0.2 \times 0.2 \times 0.34$ cm dimensions. The satellite is scheduled for launch in mid-2024 aboard the Spectrum launcher from ISAR Aerospace.

The primary mission objective is to serve as an in-orbit demonstrator and qualification of different payloads and technologies in space, such as the demonstrators of the UC3M (Universidad Carlos III de Madrid), or the instruments from the company Hydra Space Systems.

This satellite is a predecessor of another two missions, the UPMSat-2 and the UPMSat, two larger satellites also developed mainly by the IDR/UPM. These satellites were caracterized as small-sats, as they were around 0.5 x0.5x 0.6 m each and rounded the 50 kg. However, the mission they were made to accomplish was almost the same: scientific in-orbit demonstrators that to qualify different payloads in a sun-synchronous LEO orbit.

3.2   Thermal Design of the UPMSat3

The thermal design of the UPMSat3 has also been developed in the IDR/UPM and

Chapter 4

Conclusions

Appendices

Anexo A

Título del anexo

Aquí puedes meter la información que no sea imprescindible en el cuerpo del trabajo pero si que interese que esté en el documento.